Monatsh Chem (2011) 142:463–468
DOI 10.1007/s00706-011-0463-0

ORIGINAL PAPER

(*E*)-2-Benzylidenecyclanones: Part VI. Solvent effect on the UV and fluorescence properties of some chalcones and their cyclic analogues. Interaction of 4-dimethylaminochalcones with bovine and human serum albumin: a UV–vis study

Krisztina Fodor · Vladimira Tomescova · Tamás Kőszegi · Ivan Kron · Pál Perjési

Received: 14 October 2010 / Accepted: 17 February 2011 / Published online: 18 March 2011

Abstract UV–vis and fluorescence spectroscopic investigations of chalcones and cyclic chalcone analogues, (*E*)-2-(4-X-benzylidene)-1-indanones, -tetralones, and -benzosuberones with the same substitution patterns were performed in solvents with different polarity. Comparison of position of the absorption maxima of three substituted series (unsubstituted, methoxy, and dimethylamino) showed the same decreasing order indanones ≥ chalcones ≥ tetralones ≥ benzosuberones in each solvent indicating the strongest conjugation of the rigid, planar indanones. All the compounds showed positive solvatochromism, which is consistent with transitions having significant charge transfer character. The order of the observed solvent-induced bathochromic shifts of the absorption maxima was found to correlate with the donor number of the solvents. The solvent-induced shift of the emission maxima of each compound is larger than that of the absorption maxima. Recording the UV–vis spectra of the compounds in the presence of bovine and human serum albumin resulted in a slight hypsochromic shift of (*E*)-2-(4-methoxybenzylidene)- and (*E*)-2-[(4-dimethylamino)benzylidene]benzosuberone indicating changing the polar environment to a less polar one. Such an observation is in accord with an interaction of the molecules with the hydrophobic binding site(s) of the two proteins.

Keywords Cyclic chalcone analogues · Enones · UV/vis spectroscopy · Fluorescence spectroscopy · Solvatochromism · Intramolecular charge transfer

K. Fodor · P. Perjési (✉)
Institute of Pharmaceutical Chemistry,
University of Pécs, Pecs, Hungary
e-mail: pal.perjesi@aok.pte.hu

V. Tomescova · I. Kron
Department of Medical Chemistry, Biochemistry and Clinical Biochemistry, Faculty of Medicine UPJŠ, Kosice, Slovakia

T. Kőszegi
Institute of Laboratory Medicine,
University of Pécs, Pecs, Hungary

Introduction

Chalcones (**1**) are intermediary compounds of the biosynthetic pathway of a very large and widespread group of plant constituents known collectively as flavonoids [2]. Among the naturally occurring chalcones and their synthetic analogues, several compounds displayed antineoplastic activity [3]. Recently we have investigated the in vitro antineoplastic activity of several synthetic chalcones and chalcone analogues [4–6]. Among the compounds investigated (*E*)-2-(4-methoxybenzylidene)-1-benzosuberone (**4b**) and (*E*)-2-(4-dimethylaminobenzylidene)-1-benzosuberone (**4c**) (Fig. 1) had the greatest tumor cytotoxicity [4]. While investigating the mechanism of cytotoxicity of the compounds, the effect on the mitochondrial outer membrane of some methyl- and methoxy-substituted (*E*)-2-arylmethylene-1-tetralones (**3**) and (*E*)-2-arylmethylene-1-benzosuberones (**4**) were investigated by fluorescence spectroscopy [7].

Based on the previous literature, chalcones and cyclic chalcone analogues seem to be promising molecular tools to investigate the change of molecular surroundings both in solution and in biological systems [8–12]. Earlier results indicated that the ring size of the cyclic chalcone analogues has a remarkable impact on the stereochemistry and ground state electron distribution of the compounds [13–15]. Accordingly, application of cyclic chalcone analogues

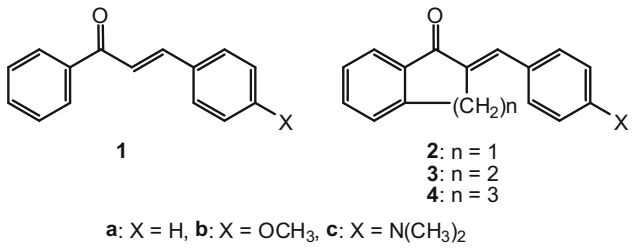

Fig. 1 Structure of the investigated chalcones **1**, and (*E*)-2-(X-benzylidene)-1-indanones **2**, -tetralones **3**, and -benzosuberones **4**

provides the possibility to investigate how the stereochemistry and ground-state electron distribution affect interaction with the molecular surroundings of this class of compounds.

In order to gain a better understanding of spectroscopic characteristics of the compounds under different molecular environments, we performed UV–vis and fluorescence spectroscopic investigations of selected 4-X-chalcones **1a**–**1c**, and the cyclic chalcone analogues (*E*)-2-(4-X-benzylidene)-1-indanones **2a**–**2c**, -tetralones **3a**–**3c**, and -benzosuberones **4a**–**4c** (Fig. 1). The compounds represent open chain (**1**) and cyclic (**2**–**4**) structures with substituents of different electron-donating capacity on their benzylidene moiety [14, 16]. This contribution is aimed to demonstrate how stereochemistry and electronic structure affects the measured UV–vis and fluorescence spectroscopic parameters in the four series of chalcones in solvents with different polarity.

Earlier results suggested that the chalcone derivatives exert their biological activities through noncovalent interactions with cellular macromolecules [4–6]. As a continuation of these previous works, we here report on UV–vis results of studies of the interaction of the investigated compounds with bovine (BSA) and human serum albumin (HSA).

Results and discussion

The peak wavelengths of the absorption spectra (λ_{max}) of the investigated compounds in cyclohexane (CHX), methanol (MeOH), acetonitrile (ACN), and dimethyl sulfoxide (DMSO) are summarized in Tables 1, 2, and 3. Selected physico-chemical properties of the used solvents are listed in Table 4. Electronic transitions in the investigated compounds lead to two absorption bands in the ultraviolet region in the spectra generally denoted as Band I (300–400 cm^{-1}) and Band II (200–300 cm^{-1}), respectively [16]. In the least polar cyclohexane the fine structure (vibrational splitting) of Band I of compounds **2a** and **2b** can be observed (Tables 1, 2). In the case of flavones, Band I is associated with the cynnamoyl moiety, whereas Band II with the benzoyl moiety of the compounds, both involving π–π^* electron transitions [16].

Comparison of position of the absorption maxima in the three series (unsubstituted as well as methoxy and dimethylamino substituted) shows the same decreasing order **2** ≥ **1** ≥ **3** ≥ **4** in each solvent, indicating the strongest conjugation of the rigid, planar compounds **2**. It is worth mentioning that a similar decreasing order of effectiveness of the transmission of substituent effects of

Table 1 UV–vis absorption maxima of compounds **1a**–**4a**

Solvent	**1a**		**2a**		**3a**		**4a**	
	λ_1 (nm)	λ_2 (nm)	λ_1 (nm)	λ_2 (nm)	λ_1 (nm)	λ_2 (nm)	λ_1 (nm)	λ_2 (nm)
CHX	226	301	228, 236	299, 312, 326	–	297	226	295
ACN	–	307	228	315	–	301	226	299
MeOH	226	309	230	321	227	305	230	302
DMSO	266	315	268	321	265	306, 320	265	305

Spectra were recorded on Secomam Anthelie light UV–vis spectrophotometer using 2.5 × 10^{-5} M solutions

Table 2 UV–vis absorption maxima of compounds **1b**–**4b**

Solvent	**1b**		**2b**		**3b**		**4b**	
	λ_1 (nm)	λ_2 (nm)	λ_1 (nm)	λ_2 (nm)	λ_1 (nm)	λ_2 (nm)	λ_1 (nm)	λ_2 (nm)
CHX	236	333	246	337, 352	237	332	234	323
ACN	239	336	246	347	245	339	238	327
MeOH	240	342	247	354	243	344	238	336
DMSO	–	348	–	356	–	348	–	336

Spectra were recorded on Secomam Anthelie light UV–vis spectrophotometer using 2.5 × 10^{-5} M solutions

Table 3 UV–vis absorption maxima of compounds **1c**–**4c**

Solvent	**1c**		**2c**		**3c**		**4c**	
	λ_1 (nm)	λ_2 (nm)	λ_1 (nm)	λ_2 (nm)	λ_1 (nm)	λ_2 (nm)	λ_1 (nm)	λ_2 (nm)
CHX	256	386	262	403	262	385	257	373
ACN	262	410	268	420	269	406	262	395
MeOH	266	421	271	431	271	419	265	404
DMSO	275	424	277	431	279	424	274	404

Spectra were recorded on Secomam Anthelie light UV–vis spectrophotometer using 1.25×10^{-5} M (**2c**) or 2.5×10^{-5} M (**1c**, **3c**, **4c**) solutions

Table 4 Properties of solvents used in this work

Solvent	Refractive index (n)[a]	Relative permittivity (ε_r)[a]	Dipole moment (μ)[b] ($\times 10^{30}$ C m)	E_T^N (kJ/mol)[c]	π^*[d]	DN[e] (kcal/mol)	AN[f]
CHX	1.426	2.02	0.0	0.025	0.00	0.0	0.0
ACN	1.344	35.94	11.8	1.926	0.66	14.1	18.9
MeOH	1.328[b]	32.66[b]	5.5	3.190	0.60	19.1	41.3
DMSO	1.479	46.71	13.5	1.859	1.00	29.8	19.3

[a] Ref. [23]

[b] Ref. [24]

[c] Ref. [19]

[d] Ref. [25]

[e] Ref. [22]

[f] Ref. [26]

some *para*-substituted derivatives **1**–**4** could be observed by SSP analysis of their IR carbonyl wavenumbers [14]. On the other hand, SSP and DSP analyses of transmission of substituent effects of the same derivatives **1**–**4** based on the ^{13}C NMR δ(C2) data showed a similar order (**2** $\approx$ **1** $\geq$ **4** $\geq$ **3**) of the obtained regression coefficients [14, 15]. Accordingly, all the methods indicated the strongest conjugation, i.e., the most planar structure of compounds **2**.

It can be seen from the molecular structures that the methoxy and the dimethylamino substituted derivatives have the same donor-acceptor type chromophore [17, 18] where the electron-donating groups (OCH_3 and $N(CH_3)_2$) are linked to the electron accepting a carbonyl group through a styrene moiety (Fig. 1). The large bathochromic shift of the Band I value of the dimethylamino substituted **1c**–**4c** relative to the respective unsubstituted **1a**–**4a** or the less powerful electron-donating methoxy substituted **1b**–**4b** typifies the donor-acceptor character of the compounds (Tables 1, 2, 3).

As is demonstrated, increasing solvent polarity causes a bathochromic shift in Band I absorption maxima of the conjugated systems (Tables 1, 2, 3). The red (bathochromic) shift is more pronounced in the dimethylamino compounds **1c**–**4c** than in the respective methoxy derivatives **1b**–**4b** and the least in the unsubstituted compounds **1a**–**4a** (Tables 1, 2, 3). The bathochromic shift in the absorption maxima with increasing solvent polarity is termed positive solvatochromism [19]. The origin of solvatochromism is a large ground-state dipole moment and a large difference dipole moment for the transition. The observed positive solvatochromism is consistent with a transition having a significant charge transfer (CT) character. As a result of the CT character of the molecules, the excited state is more dipolar than the ground state, and the electronic transition energy decreases with increasing solvent polarity [20].

Table 4 shows the most frequently used macroscopic bulk [relative permittivity (ε_r), dipole moment (μ), refractive index (n)] and molecular-microscopic [normalized Reichardt-Dimroth parameter (E_T^N), Kamlet-Taft solvent parameter (π^*), donor number (DN), and acceptor number (AN)] empirical parameters of the solvents used in this work. Due to its complexity, solvent polarity is frequently described by empirical solvent parameters derived from suitable selected reference processes, which reflect the multitude of possible solute/solvent interactions [21]. As shown in Tables 1, 2, and 3, the solvent-induced bathochromic shifts of the absorption maxima in both the methoxy (**1b**–**4b**) and the dimethylamino (**1c**–**4c**) series follow the same order: CHX < ACN < MeOH $\leq$ DMSO. Such an order of the observed red shifts of the compounds

Table 5 Molar transition energy (E_T) values (kJ/mol) of compounds **1–4** calculated from their Band I UV maxima in various solvents

Solvent	**1a**	**2a**	**3a**	**4a**	**1b**	**2b**	**3b**	**4b**	**1c**	**2c**	**3c**	**4c**
CHX	397.70	400.34	403.06	405.78	359.47	355.20	360.56	370.61	310.11	297.05	310.91	320.91
ACN	389.91	380.03	397.70	400.34	356.25	344.95	353.11	366.05	291.94	284.99	294.83	303.04
MeOH	387.40	372.91	392.47	396.36	350.01	338.16	347.96	356.25	284.32	277.75	285.70	296.30
DMSO	380.03	372.91	374.09	392.47	343.98	336.24	343.98	356.25	282.31	277.75	282.31	296.30

only correlates with the donor number (DN) [22] of the solvents. This correlation also applies to the absorption maxima of compounds **1c–4c** measured in another set of solvents [12]. The DN expresses the total interaction of the donor molecule with an acceptor molecule, including such contributions as the dipole-dipole or ion-dipole interactions as well as the binding effect caused by the availability to a free electron pair [22]. The observed correlation thus can be well explained by the dependence of stabilization of the more dipolar excited state of the molecules on the solubilization capacity of the solvents.

The absorption data of the compounds were also analyzed by means of transformation of λ_{max} (nm) values in various solvents into molar transition energies (E_T, kJ/mol) by using the following relationship [19]:

$$E_T = 119.703/\lambda_{max}$$

The E_T values signify transition energy, which also reflects the stabilization of the compounds in their ground state in a given solvent because of solvent-compound interaction. Therefore, E_T values provide a direct empirical measure of the compounds' solvation behavior. As shown in Table 5, the E_T values of the compounds show a maximum in the case of the least polar solvent cyclohexane. The rationale behind this is the same as described previously.

Steady-state fluorescence excitation and emission spectra of compounds **1a–4c** were recorded in cyclohexane, methanol, and acetonitrile. The measured excitation and emission maxima and fluorescence intensities are summarized in Tables 6, 7, and 8. As shown, measurable fluorescence of the unsubstituted compounds **1a–4a** could only be recorded in ACN solutions. On the other hand, only the dimethylamino substituted derivatives **1c–4c** had measurable fluorescence dissolved in the least polar cyclohexane (Tables 6, 7, 8). In the case of this latter series, fluorescence intensity was found to be characteristically different in the three solutions (Table 8).

Comparison of the emission maxima (λ_{em}) in the dimethylamino series (**1c–4c**) indicates a strong red shift of the maxima in the two polar solvents. The solvent-induced shift of the emission maxima of each compound is larger than that of the absorption maxima (Table 8). This suggests that the molecules are significantly solvated in the S_1 excited state, resulting in a large difference in the dipole moment between the S_1 excited state and the ground state

Table 6 Fluorescence excitation (λ_{ex}) and emission (λ_{em}) maxima and fluorescence intensities (*FI*) of compounds **1a–4a**

Solvent	**1a**			**2a**			**3a**			**4a**		
	λ_{ex} (nm)	λ_{em} (nm)	*FI*	λ_{ex} (nm)	λ_{em} (nm)	*FI*	λ_{ex} (nm)	λ_{em} (nm)	*FI*	λ_{ex} (nm)	λ_{em} (nm)	*FI*
CHX	301	–	–	311	–	–	296	–	–	295	–	–
ACN	305	365	0.4	314	370	0.3	299	370	0.8	298	360	0.2
MeOH	309	–	–	320	–	–	304	–	–	302	–	–

Spectra were recorded on a Perkin-Elmer LS50B luminescence spectrofluorimeter using 2.5×10^{-5} M solutions

Table 7 Fluorescence excitation (λ_{ex}) and emission (λ_{em}) maxima and fluorescence intensities (*FI*) of compounds **1b–4b**

Solvent	**1b**			**2b**			**3b**			**4b**		
	λ_{ex} (nm)	λ_{em} (nm)	*FI*	λ_{ex} (nm)	λ_{em} (nm)	*FI*	λ_{ex} (nm)	λ_{em} (nm)	*FI*	λ_{ex} (nm)	λ_{em} (nm)	*FI*
CHX	331	–	–	335	–	–	331	–	–	322	–	–
ACN	336	403	0.2	340	426	0.8	337	421	0.3	327	404	0.1
MeOH	341	464	2.0	353	457	16.9	343	448	0.6	332	–	–

Spectra were recorded on a Perkin-Elmer LS50B luminescence spectrofluorimeter using 2.5×10^{-5} M solutions

Table 8 Fluorescence excitation (λ_{ex}) and emission (λ_{em}) maxima and fluorescence intensities (*FI*) of compounds **1c**–**4c**

Solvent	**1c**			**2c**			**3c**			**4c**		
	λ_{ex} (nm)	λ_{em} (nm)	*FI*	λ_{ex} (nm)	λ_{em} (nm)	*FI*	λ_{ex} (nm)	λ_{em} (nm)	*FI*	λ_{ex} (nm)	λ_{em} (nm)	*FI*
CHX	382	449	2.9	402	423	20.1	382	455	1.7	372	441	1.3
					445	23.1						
ACN	409	538	698.3	420	536	506.9	405	553	51.1	393	536	58.5
MeOH	421	547	25.6	430	538	21.2	421	530	6.0	403	511	5.4

Spectra were recorded on a Perkin-Elmer LS50B luminescence spectrofluorimeter using 2.5×10^{-5} M solutions

Table 9 UV–vis absorption maxima and absorbances (*A*) of chalcones **1a**, **1b**, **1c** and their cyclic analogues **4a**, **4b**, **4c** in the respiration medium containing 1% DMSO and 1 mM sodium succinate without and in the presence of bovine serum albumin (BSA)

Compound	Without protein		With BSA ($c = 2$ μg/cm^3)		With BSA ($c = 10$ μg/cm^3)	
	λ (nm)	*A*	λ (nm)	*A*	λ (nm)	*A*
1a	312	0.346	312	0.362	311	0.462
4a	309	0.381	306	0.287	308	0.282
1b	344	0.615	346	0.461	345	0.373
4b	340	0.397	338	0.241	335	0.253
1c	270	0.546	270	0.247	268	0.245
	427	0.329	430	0.464	429	0.421
4c	271	0.486	272	0.224	272	0.252
	416	0.412	418	0.294	415	0.253

Spectra were recorded on a MultiSpec-1501 UV–vis spectrophotometer

Table 10 UV–vis absorption maxima and absorbances (*A*) of chalcones **1a**, **1b**, **1c**, and their cyclic analogues **4a**, **4b**, **4c** in the respiration medium containing 1% DMSO and 1 mM sodium succinate without and in the presence of human serum albumin (HSA)

Compound	Without protein		With HSA ($c = 2$ μg/cm^3)		With HSA ($c = 10$ μg/cm^3)	
	λ (nm)	*A*	λ (nm)	*A*	λ (nm)	*A*
1a	312	0.346	312	0.368	312	0.494
4a	309	0.381	310	0.335	307	0.311
1b	344	0.615	346	0.480	346	0.407
4b	340	0.397	340	0.251	335	0.239
1c	270	0.546	270	0.222	270	0.222
	427	0.329	430	0.448	427	0.368
4c	271	0.486	272	0.231	271	0.269
	416	0.412	416	0.319	405	0.274

Spectra were recorded on a MultiSpec-1501 UV–vis spectrophotometer

[9]. This observation is in accordance with the above-described positive solvatochromism of the compounds.

UV spectroscopic studies of the compounds in the presence of BSA and HSA ($c = 10$ μg/cm^3) indicated a hypsochromic shift of the Band I maxima of **4b** (BSA, HSA) and **4c** (HSA), indicating a change in the molecular environment of the compounds (Tables 9, 10). This observation is in accord with interaction of the molecules with the hydrophobic binding site(s) of the two proteins. Similar studies of the other investigated derivatives did not indicate such an interaction, suggesting the importance of a spatial arrangement of the electron-rich moieties of the compounds. It is worth mentioning that **4b** displayed the most pronounced tumor cell cytotoxic effects, and structure-activity relationship studies also indicated the importance of the ring size and the presence of the electron-rich aromatic substituent in the biological activity of the compounds [4, 5].

Experimental

Compounds **1a**–**4c** were synthesized, and their structures were characterized as described before [4, 13]. Their structures were characterized by IR and ^{1}H NMR spectroscopy. Their purity was checked by thin-layer chromatography (TLC) and gas chromatography (GC) methods. Other chemicals used were of the analytical grade available and, if not otherwise specified, purchased from Sigma-Aldrich (Hungary, Budapest) or Serva (Heidelberg, Germany). Compounds **1a**–**4c** were dissolved in DMSO immediately before use. The respiration medium (pH 7.4) containing EDTA (0.78 mM), $MgCl_2$ (6 mM), TRIS HCl (15 mM), KCl (0.08 mM), K_2HPO_4 (0.3 M), and KH_2PO_4 (0.3 M) was prepared using bidistilled water.

UV–vis measurements were performed on Specord M40 (Carl Zeiss Jena, Germany), Secomam Anthelie Light (Secomam, France), and MultiSpec-1501 (Shimadzu, Japan) UV–vis spectrophotometers using 1-cm path length quartz cuvettes at ambient temperature. Each UV–vis measurement except that of **2c** was performed with 2.5×10^{-5} M solutions. UV–vis spectra of **2c** were recorded with 1.25×10^{-5} M solutions.

The fluorescence (excitation and emission) spectra were run on a Perkin-Elmer LS50B Luminescence Spectrofluorimeter (Perkin Elmer, UK) using 1-cm path length quartz cuvettes at ambient temperature. The wavelength scan speed of both monochromators was 600 nm/min. Setting of the instrument's excitation slit was 10 nm and of the emission slit was 5 nm. Data processing was managed by the FL Winlab (Perkin-Elmer) software package. Measurements were done with 2.5×10^{-5} M solutions.

Interaction with BSA and HSA was studied on a MultiSpec-1501 (Shimadzu, Japan) UVis spectrophotometer using 1-cm path length quartz cuvettes at ambient temperature. Immediately before use, compounds were dissolved in DMSO and kept in the dark. The freshly prepared solutions (2.5×10^{-3} M) were diluted with the respiration medium containing 1 mM sodium succinate to a final concentration of 25 nmol/cm^3 (2.5×10^{-5} M). Concentration of DMSO in the mixtures was 1% v/v. Measurements were performed in the presence of two different BSA and HSA concentrations (2 and 10 μg/cm^3) after 60 min equilibration at room temperature in the dark.

Acknowledgments This study was supported by the Faculty of Medicine Research Fund (AOK-KA 34039-12/2009), University of Pécs. The authors express their sincere thanks to Professor Miklós Nyitrai (Department of Biophysics, University of Pécs) for providing the possibility of performing the fluorescence measurements in his laboratory.

References

1. (*E*)-2-Benzylidenecyclanones. Part V: Perjési P, Rozmer Z, Open Med Chem J (accepted)
2. Tomas-Barberan FA, Clifford MN (2000) J Sci Food Agric 80:1073
3. Go ML, Wu X, Liu XL (2005) Curr Med Chem 12:483
4. Dimmock JR, Kandepu NM, Nazarali AJ, Kowalchuk TP, Motaganahalli N, Quail JW, Mykytiuk P, Audette GF, Prasad L, Perjési P, Allen TM, Santos CL, Szydlowski J, De Clercq E, Balzarini J (1999) J Med Chem 42:1358
5. Dimmock JR, Zello GA, Oloo EO, Quail JW, Kraatz H-B, Perjési P, Aradi F, Takács-Novák K, Allen TM, Santos CL, Balzarini J, DeClerq E, Stables JP (2002) J Med Chem 45:3103
6. Perjési P, Das U, DeClercq E, Balzarini J, Kawase M, Sakagami H, Stables JP, Loránd T, Rozmer Z, Dimmock JR (2008) Eur J Med Chem 43:839
7. Tomečková V, Perjési P, Guzy J, Kušnír J, Chovanova Z, Chavkova Z, Marekova M (2004) J Biochem Biophys Meth 61:135
8. Pengfei W, Shikang W (1994) J Photochem Photobiol A 77:127
9. Pengfei W, Shikang W (1995) J Photochem Photobiol A 86:109
10. Hui W, Minghua M, Hongzhi X, Yu F, Xiaohong Z, Shikang W (2003) Arkivoc 2003(ii):173
11. Fayed TA, Awad MK (2004) Chem Phys 303:317
12. Tomeckova V, Poskrobova M, Stefanisinova M, Perjési P (2009) Spectrochim Acta Part A 74:1242
13. Perjési P, Nusser T, Tarczay Gy, Sohár P (1999) J Mol Struct 479:13
14. Perjési P, Perjessy A, Kolehmainen E, Ősz E, Samalikova M, Linnanto J, Virtanen E (2004) J Mol Struct 697:41
15. Perjési P, Linnanto J, Kolehmainen E, Ősz E, Virtanen E (2005) J Mol Struct 740:81
16. Wolfbeis OS, Begum M, Geiger H (1984) Z Naturforsch 39b:231
17. Asiri AM (2003) Bull Korean Chem Soc 24:426
18. Zhang C-H, Chen Z-B, Jiang Y-B (2004) Spectrochim Acta Part A 60:2729
19. Reichardt C (1994) Chem Rev 94:2319
20. Wang H, Borguet E, Eisenthal KB (1997) J Phys Chem A 101:713
21. Reichardt C (2004) Pure Appl Chem 76:1903
22. Gutmann V (1967) Coord Chem Rev 2:239
23. Abboud JLM, Notorio R (1999) Pure Appl Chem 71:645
24. Ballistreri FP, Fortuna CG, Musumarra G, Pavone D, Scire S (2002) Arkivoc 2002(xi):54
25. Laurence C, Nicolet P, Dalati MT, Abboud J-LM, Notorio R (1994) J Phys Chem 98:5807
26. Mayer U, Gutmann V, Gerger W (1975) Monatsh Chem 106:1235